Dipole-pion cross section in the saturation regime

G. R. Boroun*
Physics Department, Razi University, Kermanshah 67149, Iran

B. Z. Kopeliovich†
Departamento de Física, Universidad Técnica Federico Santa María, Avenida España 1680, Valparaíso, Chile

(Received 18 April 2025; accepted 27 June 2025; published 15 July 2025)

The scale-dependent dipole-pion cross section is analyzed as a function of the dipole size r and the impact parameter b. This analysis relies on the Dokshitzer-Gribov-Lipatov-Altarelli-Parisi (DGLAP) evolution equation in $\mu \sim 1/r + \mu_0$ at the next-to-leading order (NLO) approximation, with a specific initial condition at μ_0. The dipole-pion cross section at small Bjorken variable β is being considered over a wide range of transverse separations $\mathbf{r}$. Using the Laplace transformation technique, we describe the determination of the dipole-pion cross section based on the gluon distribution at the initial scale μ_0 within a kinematic region characterized by low values of the Bjorken variable β. We found that geometric scaling for the dipole-pion cross section holds approximately within a wide kinematic region of rQ_s. The cross section saturates at large dipole sizes.

DOI: 10.1103/y567-4tb6

I. INTRODUCTION

The color-dipole model and dipole cross section were initially introduced in Ref. [1] to explain that the interaction eigenstates in quantum chromodynamics (QCD) are the eigenstates of the interaction amplitude with specific values of the transverse dipole moment. Assuming that gluons in hadrons are concentrated in small areas occupying only about 10% of the light hadron's total area can be beneficial in high-energy hadronic collisions as mentioned in Ref. [2]. This concept was further developed beyond the "frozen" dipole approximation in a perturbative manner, investigating the influence of quantum coherence effects on the transverse momentum distribution of photons and gluons radiated by a quark moving through nuclear matter in Ref. [3]. Additionally, the nonperturbative interaction for light-cone fluctuations involving quarks and gluons is discussed in Ref. [4].

In the dipole picture [5], the virtual photon γ^* splits into a quark-antiquark pair (a dipole) with virtuality Q^2 exchanged between the electron and target. The dipole, with the transverse size $\mathbf{r}$ between the quark and antiquark, interacts with the pion cloud of the proton in the leading neutrons[1] [6,7]. The quark and antiquark in this dipole, carry a fraction z and $1-z$ of the photon's longitudinal momentum respectively, probing the pion cloud of the proton in the inclusive $\gamma^*\pi^*$ cross section in leading neutron events $e + p \to e' + X + n$. The leading neutron production in Deep-Inelastic Scattering (DIS) is a method to measure the dipole cross section of the pion, $\sigma^{\pi}_{\rm dip}(x, \mathbf{r})$ [8].

The cross section of the $\gamma^*\pi^*$ interaction is directly proportional to the differential cross section for $\gamma^* p$ according to the following formula [9]

$$\sigma^{\gamma^*\pi^*}(\hat{W}^2, Q^2) = \frac{1}{f_{\pi/p}(x_L, t)} \frac{d^2\sigma(W, Q^2, x_L, t)}{dx_L dt}, \quad (1)$$

where $f_{\pi/p}$ represents the flux of pions emitted by the proton and explains the splitting of a proton into a πn system. This flux is well known and can be calculated using chiral effective theory. In the chiral approach [10], the proton is depicted as a combination of states in meson-cloud models

$$|p\rangle \to \sqrt{1-a-b}|p_0\rangle + \sqrt{a}\left(-\sqrt{\frac{1}{3}}|p_0\pi^0\rangle + \sqrt{\frac{2}{3}}|n_0\pi^+\rangle + \cdots\right), \quad (2)$$

*Contact author: boroun@razi.ac.ir
†Contact author: boris.kopeliovich@usm.cl

Published by the American Physical Society under the terms of the Creative Commons Attribution 4.0 International license. Further distribution of this work must maintain attribution to the author(s) and the published article's title, journal citation, and DOI. Funded by SCOAP³.

[1]The leading neutrons have been known as neutron production in deep-inelastic scattering (DIS) on a proton where neutrons carry a large fraction of the proton's longitudinal momentum in the forward direction.

with $a = 0.24$ and $b = 0.12$. The variables in Eq. (1) are as follows: t represents the four-momentum transfer squared at the proton vertex, and x_L represents the longitudinal momentum fraction carried by the outgoing neutron. These variables are related to the transverse momentum of the neutron, p_T, as

$$t \simeq -\frac{p_T^2}{x_L} - (1 - x_L)\left(\frac{m_n^2}{x_L} - m_p^2\right), \tag{3}$$

with the neutron and proton masses (i.e., m_n and m_n). The center-of-mass (COM) energies for the photon-proton and photon-pion systems are denoted by W and $\hat{W}$ respectively, where $\hat{W}^2 = (1 - x_L)W^2$.

The phenomenon of gluon saturation[2] due to the nonlinear effects was implemented in the dipole picture where has been extended by authors in Refs. [11–14]. The color dipole model in the context of saturation was formulated in Ref. [15][3] and later extended by parametrization models incorporating saturation physics in Refs. [16–20]. Saturation and hadron cross sections at very high energies discussed in Refs. [21,22]. At high energies the small-x gluons in a hadron wave function should form a color glass condensate (CGC) [23,24], which is characterized by gluon saturation and the saturation scale Q_s. This scale determines the critical line separating the linear and saturation regimes of QCD dynamics.

The total $\gamma^*\pi^*$ cross section, using the optical theorem, is related to the dipole-pion cross section as

$$\sigma_{L,T}^{\gamma^*\pi^*}(\beta, Q^2) = \int d^2\mathbf{r} \int_0^1 \frac{dz}{4\pi} |\Psi_{L,T}^f(\mathbf{r}, z; Q^2)|^2 \sigma_{\rm dip}^{\pi}(\beta, \mathbf{r}), \tag{4}$$

where $\Psi_{L,T}(\mathbf{r}, z; Q^2)$ are the appropriate spin averaged light-cone wave functions of the photon, which give the probability for the occurrence of a $(q\bar{q})$ fluctuation of transverse size with respect to the photon polarization [25]. The Bjorken variable scaled for the photon-pion system is given by

$$\beta = \frac{Q^2 + m_f^2}{\hat{W}^2 + Q^2} = \frac{Q^2 + m_f^2}{(1 - x_L)W^2 + Q^2}, \tag{5}$$

where m_f is the active quark mass defined by the mass of the charm quark with the number of active flavors $n_f = 4$. The dipole-virtual pion cross section was proposed by the Golec-Biernat-Wüsthoff (GBW) model [16] as

$$\sigma_{\rm dip}^{\pi}(\beta, \mathbf{r}) = \sigma_0(1 - e^{-r^2 Q_s^2(\beta)/4}), \tag{6}$$

where $Q_{\rm sat}(\beta)$ plays the role of saturation and is defined by the form $Q_{\rm sat}^2(\beta) = Q_0^2(x_0/\beta)^\lambda$ with $Q_0^2 = 1$ GeV^2. The geometric scaling [26] implies that the pion cross section depends only on one dimensionless variable $rQ_s(\beta)$ (for all values of r and β), as shown by

$$\sigma_{\rm dip}^{\pi}(\beta, r) = \sigma_{\rm dip}^{\pi}(rQ_s(\beta)). \tag{7}$$

The pion cross section can be defined by the following form

$$\sigma_{\rm dip}^{\pi}(\beta, r) = \int d^2b \frac{d\sigma_{\rm dip}^{\pi}}{d^2b}, \tag{8}$$

which contains all information about the target and the strong interaction physics with the impact parameter (IP), b.

The dipole pion cross section at a given impact parameter b (bSat model or IP-Sat model [17,18]) contains the DGLAP equation [27–29] for the evolution of the gluon density at large scales

$$\frac{d\sigma_{\rm dip}^{\pi}}{d^2b}(\mathbf{b}, \mathbf{r}, \beta) = 2\left[1 - \exp\left(-\frac{\pi^2 r^2 \alpha_s(\mu^2)\beta g(\beta, \mu^2) T_\pi(\mathbf{b})}{2N_c}\right)\right], \tag{9}$$

with $N_c = 3$, $\mu^2 = C/r^2 + \mu_0^2$ where μ^2 is the hard scale, and the parameters C and μ_0^2 are obtained from the fit to the DIS data as summarized in [7,30]. The Gaussian form of the function $T_\pi(\mathbf{b})$ is determined from the fit to the data as

$$T_\pi(\mathbf{b}) = \frac{1}{2\pi B_\pi} \exp\left(-\frac{b^2}{2B_\pi}\right). \tag{10}$$

The parameter B_π is the width of the pion and is chosen to be $B_\pi = 2$ GeV^{-2} from the Belle measurements [31].

Since the free parameters depend on the leading neutron structure function data or the inclusive proton data, we can consider the ratio of dipole cross sections at small x given by

$$R_q = \frac{\sigma_{\rm dip}^{\pi}(r, \beta)}{\sigma_{\rm dip}^{p}(r, \beta)}, \tag{11}$$

or

$$R_q = \frac{\frac{d\sigma_{\rm dip}^{\pi}}{d^2b}(\mathbf{b}, \mathbf{r}, \beta)}{\frac{d\sigma_{\rm dip}^{p}}{d^2b}(\mathbf{b}, \mathbf{r}, \beta)}. \tag{12}$$

In a constituent quark picture and the color dipole BFKL-Regge expansion model [32], R_q represents the ratio of

[2]Gluon saturation is a phenomenon in QCD where, at high energies, the growth of the gluon density inside a hadron saturates due to the nonlinear interactions of gluons.

[3]In the large-N_c approximation, a Fock component containing gluons can be replaced by a multidipole state.

valence quarks in the pion and proton i.e., $R_q = \frac{2}{3}$. The value $R_q = \frac{1}{2}$ is acceptable as studied in Ref. [8].

In this paper, we extend the method using a Laplace transform technique and obtain an analytical method for the solution of the dipole-pion cross section in terms of the known initial condition in the kinematical region of low values of the Bjorken variable β.

II. FORMALISM

The color dipole-pion cross section in the bSat model is given by

$$\frac{d\sigma^{\pi}_{\rm dip}}{d^2b}(\mathbf{b},\mathbf{r},\beta) = 2[1-\exp(-F_{\rm DGLAP}(\mathbf{b},\mathbf{r},\beta))], \tag{13}$$

where

$$F_{\rm DGLAP}(\mathbf{b},\mathbf{r},\beta) = \frac{\pi^2 r^2 \alpha_s(\mu^2)\beta g(\beta,\mu^2) T_\pi(\mathbf{b})}{2N_c}. \tag{14}$$

The function $F_{\rm DGLAP}$ is applicable in the DGLAP evolution equation where the gluon density is dominant at low x. Therefore we find

$$\frac{\partial F_{\rm DGLAP}(\mathbf{b},\mathbf{r},\beta)}{\partial r} = -\alpha_s(\mu^2) r^2 \frac{\partial}{\partial r}\left(\frac{1}{\alpha_s(\mu^2) r^2}\right) F_{\rm DGLAP}(\mathbf{b},\mathbf{r},\beta) - \frac{2C}{r^3\mu^2}\int_\beta^1 \frac{\beta}{\gamma^2} d\gamma \sum_{n=1}\left(\frac{\alpha_s(\mu^2)}{2\pi}\right)^{(n)} P^{(n)}_{gg}\left(\frac{\beta}{\gamma}\right) F_{\rm DGLAP}(\mathbf{b},\mathbf{r},\gamma), \tag{15}$$

where n represents the order of α_s. After some rearranging, we find an evolution equation in terms of r

$$dF_{\rm DGLAP}(\mathbf{b},\mathbf{r},\beta) = F_{\rm DGLAP}(\mathbf{b},\mathbf{r},\beta)\left[\frac{2}{r} + \frac{d\ln\alpha_s(r)}{dr}\right]dr - \frac{2C}{r^3\left(\frac{C}{r^2}+\mu_0^2\right)}dr\int_\beta^1 \frac{\beta}{\gamma^2} d\gamma \sum_{n=1}\left(\frac{\alpha_s(\mu^2)}{2\pi}\right)^{(n)}$$
$$\times P^{(n)}_{gg}\left(\frac{\beta}{\gamma}\right) F_{\rm DGLAP}(\mathbf{b},\mathbf{r},\gamma). \tag{16}$$

We can rewrite the above evolution equation of the dipole-pion cross section in the bSat model in terms of the variables $\upsilon = \ln(1/\beta)$ and r instead of β and r using the notation $\hat{F}_{\rm DGLAP}(\mathbf{b},\upsilon,r) \equiv F_{\rm DGLAP}(\mathbf{b},e^{-\upsilon},r)$ as

$$d\hat{F}_{\rm DGLAP}(\mathbf{b},\upsilon,\mathbf{r}) = \hat{F}_{\rm DGLAP}(\mathbf{b},\upsilon,\mathbf{r})\left[\frac{2}{r} + \frac{d\ln\alpha_s(r)}{dr}\right]dr - \frac{2C}{r^3\left(\frac{C}{r^2}+\mu_0^2\right)}dr\int_0^\upsilon e^{-(\upsilon-w)} \sum_{n=1}\left(\frac{\alpha_s(\mu^2)}{2\pi}\right)^{(n)}$$
$$\times P^{(n)}_{gg}(\upsilon-w)\hat{F}_{\rm DGLAP}(\mathbf{b},\mathbf{r},w)dw, \tag{17}$$

By using the Laplace transform method developed in detail in [33–37] as $\mathcal{L}[\hat{F}_{\rm DGLAP}(\mathbf{b},\upsilon,\mathbf{r});s] \equiv F_{\rm DGLAP}(\mathbf{b},s,\mathbf{r})$ and the fact that the Laplace transform of a convolution factors is simply the ordinary product of the Laplace transform of the factors, we find

$$F_{\rm DGLAP}(\mathbf{b},s,r) = F_{\rm DGLAP}(\mathbf{b},s,r_0)\left(\frac{r}{r_0}\right)^2 \frac{\alpha_s(r)}{\alpha_s(r_0)}\exp\left[-\int_{r_0}^r \frac{2C}{\xi^3\left(\frac{C}{\xi^2}+\mu_0^2\right)}\sum_{n=1}\left(\frac{\alpha_s(\xi)}{2\pi}\right)^{(n)} h^{(n)}_{gg}(s)d\xi\right]. \tag{18}$$

To find the inverse Laplace transform of the factors, we find that

$$\hat{F}_{\rm DGLAP}(\mathbf{b},\upsilon,r) = \int_0^\upsilon \hat{\eta}(\mathbf{b},w,r,r_0)\hat{J}(\upsilon-w,\alpha_s(r))dw, \tag{19}$$

where

$$\hat{\eta}(\mathbf{b},\upsilon,r,r_0) = \hat{F}_{\rm DGLAP}(\mathbf{b},\upsilon,r_0)\left(\frac{r}{r_0}\right)^2 \frac{\alpha_s(r)}{\alpha_s(r_0)}. \tag{20}$$

The inverse Laplace transform of the coefficients $h^{(n)}_{gg}(s)$ in Eq. (18) is straightforward, keeping the $1/s$ terms of the coefficients at the high-energy region as

$$\hat{J}(\upsilon,\alpha_s(r)) = \delta(\upsilon) + \frac{\sqrt{-\phi}}{\sqrt{\upsilon}}\mathrm{I}_1(2\sqrt{-\phi}\sqrt{\upsilon}), \tag{21}$$

where[4]

$$\phi = \frac{2C_A}{2\pi}\int_{r_0}^{r}\frac{2C\alpha_s(r)}{r^3\left(\frac{C}{r^2}+\mu_0^2\right)}dr + \frac{(12C_FT_f - 46C_AT_f)}{9(2\pi)^2}\int_{r_0}^{r}\frac{2C\alpha_s^2(r)}{r^3\left(\frac{C}{r^2}+\mu_0^2\right)}dr, \tag{22}$$

with $C_F = \frac{N_c^2-1}{2N_c}$, $T_f = \frac{1}{2}n_f$ and $C_A = 3$. Transforming back in to β space, $F_{\rm DGLAP}(\mathbf{b},\beta,r)$ is given by

$$F_{\rm DGLAP}(\mathbf{b},\beta,r) = \left(\frac{r}{r_0}\right)^2\frac{\alpha_s(r)}{\alpha_s(r_0)}\left[F_{\rm DGLAP}(\mathbf{b},\beta,r_0) + \int_\beta^1 F_{\rm DGLAP}(\mathbf{b},\gamma,r_0)\frac{\sqrt{-\phi}}{\sqrt{\ln\frac{\gamma}{\beta}}}\mathrm{I}_1\left(2\sqrt{-\phi}\sqrt{\ln\frac{\gamma}{\beta}}\right)\frac{d\gamma}{\gamma}\right], \tag{23}$$

where

$$F_{\rm DGLAP}(\mathbf{b},\beta,r_0) = \frac{\pi^2 r_0^2\alpha_s(r_0)\beta g(\beta,r_0)T_\pi(\mathbf{b})}{2N_c}, \tag{24}$$

and the initial gluon distribution at the scale $\mu_0^2 = 1.1$ GeV^2 is defined in the form [7]

$$\beta g(\beta,\mu_0^2) = A_g\beta^{-\lambda_g}(1-\beta)^6, \tag{25}$$

where parameters in the bSat model are motivated by the leading neutron structure function HERA data for $\beta \le 0.01$ [6,7]. Therefore, the evolution of the color dipole-pion cross section in the bSat model is defined from an exclusive measurement of $e + p \to e + J/\Psi + \pi + n$ by the following form

$$\frac{1}{2}\frac{d\sigma_{\rm dip}^{\pi}}{d^2b}(\mathbf{b},\mathbf{r},\beta) = 1 - \exp\left\{-\left(\frac{r}{r_0}\right)^2\frac{\alpha_s(r)}{\alpha_s(r_0)}\left[F_{\rm DGLAP}(\mathbf{b},\beta,r_0) + \int_\beta^1 F_{\rm DGLAP}(\mathbf{b},\gamma,r_0)\frac{\sqrt{-\phi}}{\sqrt{\ln\frac{\gamma}{\beta}}}\mathrm{I}_1\left(2\sqrt{-\phi}\sqrt{\ln\frac{\gamma}{\beta}}\right)\frac{d\gamma}{\gamma}\right]\right\}. \tag{26}$$

The Bjorken scaling in the photon-proton scattering in the dipole picture is given by

$$x = \frac{(\mu^2+m_c^2)\beta(1-x_L)}{(1-\beta x_L)\mu^2 + m_c^2}, \tag{27}$$

where

$$\beta = \frac{\mu^2+m_c^2}{(1-x_L)W^2+\mu^2}, \tag{28}$$

with $m_c = 1.3$ GeV and $x_L = 0.6$. In this section, we have summarized the Laplace transform method for obtaining an analytical solution for the dipole-pion cross section. Starting with the explicit form of the dipole-pion cross section [i.e., Eq. (26)], we will now extract numerical results for small β across a wide range of μ^2 values. This will be done using the initial gluon distribution[5] at the scale μ_0^2 in the next section.

III. RESULTS AND CONCLUSION

The free parameters for the pion and proton are selected from the fit results in Refs. [7,30,40], as summarized in Table I. The QCD parameter Λ for four active flavors has been determined as $\alpha_s(M_z^2) = 0.1166$ resulting in $\Lambda^{\rm LO}_{nf=4} = 136.8$ MeV and $\Lambda^{\rm NLO}_{nf=4} = 284.0$ MeV. Table I displays the free parameters for the pion [7,30] and proton [40]. The dipole-pion cross sections, $\frac{d\sigma_{\rm dip}^{\pi}}{2d^2b}$, are plotted in Fig. 1 over a wide range of the dipole size r in the bSat model at different values of the scaled Bjorken variable $\beta = 10^{-2}$ and 10^{-4} with the impact parameters $b = 0$ and 2 GeV^{-1}.

In Fig. 1 (left-hand side), the dipole-pion cross sections are shown at $\beta = 10^{-2}$ (upper panel) and $\beta = 10^{-4}$ (lower panel) as a function of dipole size r. The dipole-pion cross sections saturate for large dipole sizes and increase toward lower dipole sizes as the Bjorken scaling decreases.

TABLE I. Free parameters for pion [7,30] and proton [40].

...	A_g	λ_g	C	μ_0^2 [GeV^2]	B [GeV^{-2}]
Proton	1.350	0.079	0.380	1.73	4.0
Pion	1.208	0.060	1.453	1.10	2.3

[4] $I_1(x)$ is the Bessel function.

[5] In the Jefferson Lab Angular Momentum (JAM) Collaboration, the pion's parton distribution functions (PDFs) have been studied within a Bayesian Monte Carlo framework with threshold resummation and transverse momentum (p_T) at the scales $\mu = \mu_0 = m_c$ and $\mu^2 = 10$ GeV^2. These finding have been reported in Refs. [38,39].

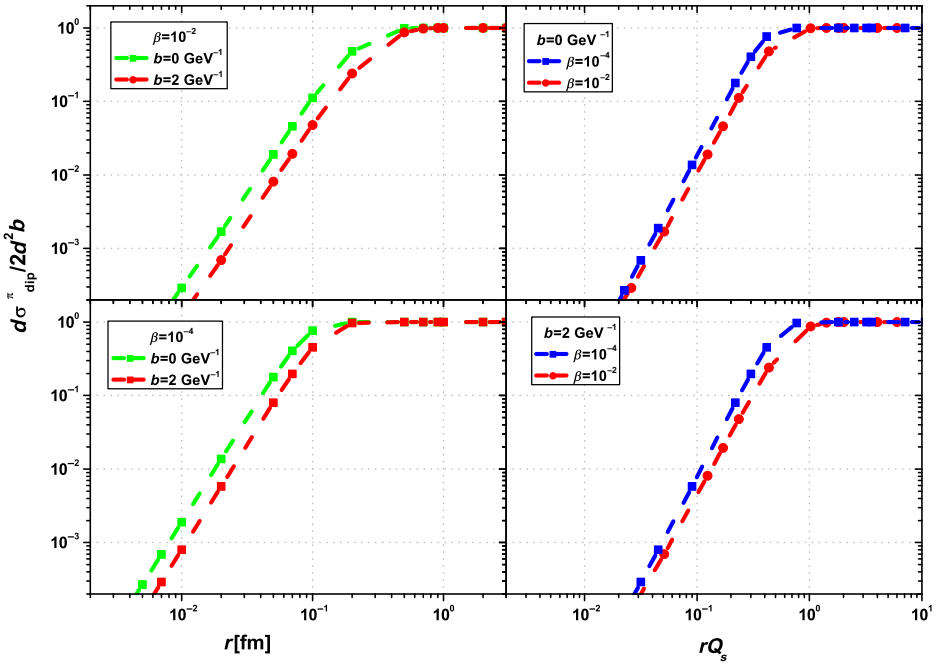


FIG. 1. Dipole-pion cross section in the bSat model as a function of r (left panel) and rQ_s (right panel) for $\beta = 10^{-2}$ and 10^{-4} at the impact parameters $b = 0$ and 2 GeV^{-1}. Left panel (upper): $\beta = 10^{-2}$ and $b = 0$ GeV^{-1} (green-square) and $b = 2$ GeV^{-1} (red-circle). Left panel (lower): $\beta = 10^{-4}$ and $b = 0$ GeV^{-1} (green-square) and $b = 2$ GeV^{-1} (red-circle). Right panel (upper): $b = 0$ GeV^{-1} and $\beta = 10^{-4}$ (blue-square) and $\beta = 10^{-2}$ (red-circle). Right panel (lower): $b = 2$ GeV^{-1} and $\beta = 10^{-4}$ (blue-square) and $\beta = 10^{-2}$ (red-circle).

The impact parameters (i.e., $b = 0$ and 2 GeV^{-1}) affect the dipole-pion cross sections at various values of r. In Fig. 1 (right-hand side), the dipole-pion cross sections in the bSat model converge into a single curve when plotted against the dimensionless variable rQ_s. The saturation formalism[6] of the dipole-pion cross section leads to improved results because the evolution of the cross section due to the Laplace transform becomes a function of a single variable, rQ_s, for almost all values of r with different β at $b = 0$ and 2 GeV^{-1} in the bSat model.

Indeed, we observe that the presence of geometric scaling in the GBW model is illustrated in the dipole-pion cross sections. All the curves from the left plot with different β and b values merge into a single curve when the dipole-pion cross section is plotted against the dimensionless variable rQ_s. This shows that the dipole cross section is indeed a function of a single dimensionless variable and is in line with the GBW model. Indeed, the dipole pion cross sections resulting from the evolution method based on the Laplace transform do not break the geometrical scaling in a wide range of rQ_s. In Ref. [7], the author demonstrates that the dipole cross section for the bSat model with different β values does not merge into a single curve when plotted against the dimensionless variable rQ_s due to the breaking of geometric scaling. The author in Ref. [7] suggests that this is because of the explicit DGLAP evolution of the gluon density in the bSat model where the gluon density is evaluated at a scale $\mu \sim 1/r + \mu_0$. We improve the results by addressing the breaking of geometrical scaling caused by the DGLAP evolution based on the Laplace transform, as shown in the right panel of Fig. 1.

The values of R_q predicted from the ratio $\frac{d\sigma^{\pi}_{\rm dip}}{d^2b}(\mathbf{b},\mathbf{r},\beta)/\frac{d\sigma^{p}_{\rm dip}}{d^2b}(\mathbf{b},\mathbf{r},\beta)$ in a wide range of dipole sizes r in the bSat model at different values of the scaled Bjorken variable $\beta = 10^{-2}$ and 10^{-4} with impact parameters $b = 0$ and 2 GeV^{-1} are illustrated in Fig. 2. This ratio varies over a wide range of dipole sizes r [7,8] and is independent of β at large and low values of r (left panel of Fig. 2). It is observed that the saturation scale increases toward lower values of r as β decreases. The behavior of R_q depends on the impact parameter b at small values of r and saturates at large values of r. The minimum values of R_q are obtained due to the β and b values in Table II.

In Fig. 2 (left-hand side), R_q is plotted at $\beta = 10^{-2}$ (upper panel) and $\beta = 10^{-4}$ (lower panel) as a function of dipole size r. R_q saturates at large dipole sizes, with saturation increasing toward lower dipole sizes as the Bjorken scaling decreases. In Fig. 2 (right-hand side), we observe that the behavior of R_q is plotted independently of β at both large and small values of r for the impact

[6]An important property of the saturation formalism is the geometric scaling phenomenon, which means that the scattering amplitude and corresponding cross sections can scale on the dimensionless scale rQ_s.

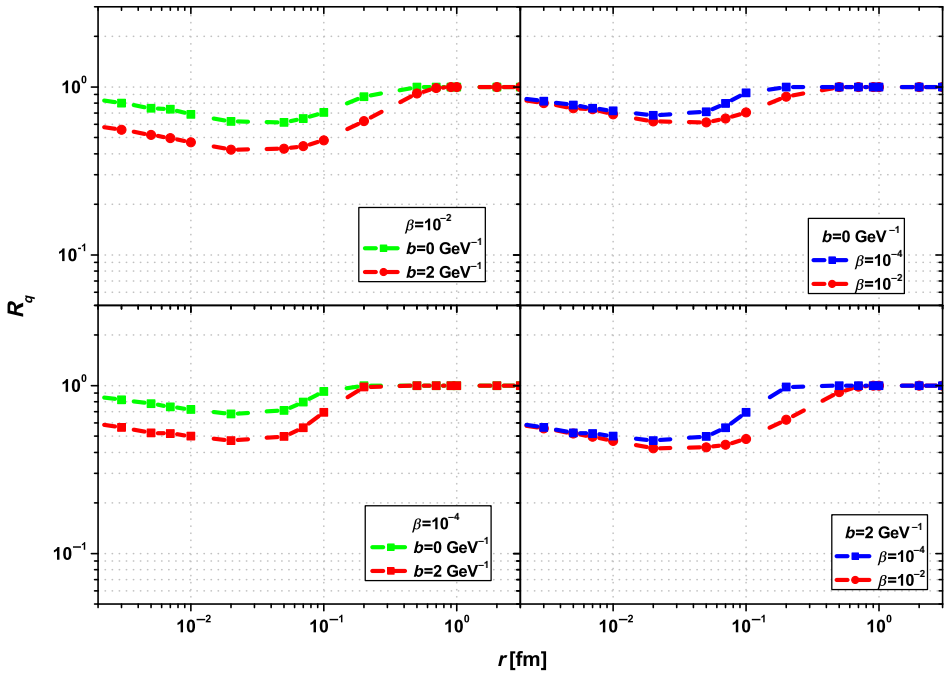


FIG. 2. The ratio $R_q = \frac{d\sigma^{\pi}_{\rm dip}}{d^2b}(\mathbf{b},\mathbf{r},\beta)/\frac{d\sigma^{p}_{\rm dip}}{d^2b}(\mathbf{b},\mathbf{r},\beta)$ is plotted as a function of r for $\beta = 10^{-2}$ and 10^{-4} at the impact parameters $b = 0$ and 2 GeV^{-1}. Left panel (upper): $\beta = 10^{-2}$ and $b = 0$ GeV^{-1} (green square) and $b = 2$ GeV^{-1} (red circle). Left panel (lower): $\beta = 10^{-4}$ and $b = 0$ GeV^{-1} (green square) and $b = 2$ GeV^{-1} (red circle). Right panel (upper): $b = 0$ GeV^{-1} and $\beta = 10^{-4}$ (blue square) and $\beta = 10^{-2}$ (red circle). Right panel (lower): $b = 2$ GeV^{-1} and $\beta = 10^{-4}$ (blue square) and $\beta = 10^{-2}$ (red circle).

TABLE II. Minimum values of R_q into r ($0.01 < r < 0.07$ fm).

Min	β	$b = 0$ GeV^{-1}	$b = 2$ GeV^{-1}
R_q	10^{-2}	~0.61	~0.42
R_q	10^{-4}	~0.68	~0.47

parameters $b = 0$ (upper) and 2 GeV^{-1} (lower). This value depends on β at moderate r ($2 \times 10^{-2} \lesssim r \lesssim 7 \times 10^{-1}$ fm) as the impact parameter increases.

In conclusion, we have discussed the evolution of the dipole-pion cross section using the Laplace transform method in the bSat model. This evolution is presented as a function of the dipole size and the scaled Bjorken variable β. This method can successfully describe the behavior of the dipole-pion cross sections in terms of the impact parameter at small β (Fig. 1, left). The scaling behavior in the bSat model is shown at large and small dipole sizes, similar to the GBW model. These results in rQ_s (Fig. 1, right), which are independent of the impact parameter and the scaled Bjorken variable, show that the evolution of DGLAP based on the Laplace transform into the initial scale plays a dominant role in the dipole-pion cross sections, as the results show a geometrical scaling in a wide range of rQ_s.

The ratio R_q in the bSat model depends on the impact parameter at small dipole sizes and is scaled at large dipole sizes (Fig. 2). This ratio varies between the values $0.4 < R_q \leq 1$ over a wide range of r. The behavior of the ratio R_q over this range of r depends on the structure of the proton, from the valence quarks to a multiquark in the proton. Quantum fluctuations in the proton at small dipole sizes interact with the quarks and antiquarks in the meson cloud of the proton, depending on the flavor asymmetric and flavor symmetric sea [8].

ACKNOWLEDGMENTS

The work of B. K was supported in part by Grant ANID - Chile FONDECYT 1231062, by ANID PIA/APOYO AFB230003.

DATA AVAILABILITY

No data were created or analyzed in this study.

[1] A. B. Zamolodchikov, B. Z. Kopeliovich, and L. I. Lapidus, Pis'ma Zh. Eksp. Teor. Fiz. **33**, 612 (1981) [Sov. Phys. JETP Lett. **33**, 595 (1981)].
[2] B. Z. Kopeliovich, I. K. Potashnikova, B. Povh, and I. Schmidt, Phys. Rev. D **76**, 094020 (2007).
[3] B. Z. Kopeliovich, A. Schäfer, and A. V. Tarasov, Phys. Rev. C **59**, 1609 (1999).
[4] B. Z. Kopeliovich, A. Schäfer, and A. V. Tarasov, Phys. Rev. D **62**, 054022 (2000).
[5] N. N. Nikolaev and B. G. Zakharov, Phys. Lett. B **332**, 184 (1994).
[6] A. Kumar and T. Toll, Phys. Rev. D **105**, 114045 (2022).
[7] A. Kumar, Phys. Rev. D **107**, 034005 (2023).
[8] B. Z. Kopeliovich, I. K. Potashnikova, B. Povh, and I. Schmidt, Phys. Rev. D **85**, 114025 (2012).
[9] F. Carvalho, V. P. Gonçalves, D. Spiering, and F. S. Navarra, Phys. Lett. B **752**, 76 (2016).
[10] A. W. Thomas, W. Melnitchouk, and F. M. Steffens, Phys. Rev. Lett. **85**, 2892 (2000).
[11] V. P. Goncalves, F. S. Navarra, and D. Spiering, Phys. Rev. D **93**, 054025 (2016).
[12] F. Carvalho, V. P. Gonccalves, F. S. Navarra, and D. Spiering, Phys. Rev. D **103**, 034021 (2021).
[13] J. T. Amaral and V. M. Becker, Phys. Rev. D **97**, 094026 (2018).
[14] B. Z. Kopeliovich, I. K. Potashnikova, and I. Schmidt, Phys. Rev. C **81**, 035204 (2010).
[15] A. H. Mueller, Nucl. Phys. **B415**, 373 (1994) **B437**, 107 (1995).
[16] K. Golec-Biernat and M. Wüsthoff, Phys. Rev. D **59**, 014017 (1998).
[17] H. Kowalski and D. Teaney, Phys. Rev. D **68**, 114005 (2003).
[18] H. Kowalski, L. Motyka, and G. Watt, Phys. Rev. D **74**, 074016 (2006).
[19] F. Ferreiro, E. Inacu, K. Itakura, and McLerran, Nucl. Phys. **A710**, 373 (2002).
[20] A. Kovner and U. A. Wiedemann, Phys. Lett. B **551**, 311 (2003).
[21] F. Carvalho, F. O. Duraes, F. S. Navarra, and V. P. Goncalves, Acta Phys. Pol. B **39**, 2511 (2008).
[22] A. Morreale and F. Salazar, Universe **7**, 312 (2021).
[23] E. Iancu and R. Venugopalan, *Quark-Gluon Plasma 3* (2004), pp. 249–363, 10.1142/9789812795533_0005.
[24] J. Jalilian-Marian and Y. V. Kovchrgov, Prog. Part. Nucl. Phys. **56**, 104 (2006).
[25] J. T. Amaral, D. A. Fagundes, and M. V. T. Machado, Phys. Rev. D **103**, 016013 (2021).
[26] A. M. Stasto, K. J. Golec-Biernat, and J. Kwiecinski, Phys. Rev. Lett. **86**, 596 (2001).
[27] Yu. L. Dokshitzer, Sov. Phys. JETP **46**, 641 (1977).
[28] G. Altarelli and G. Parisi, Nucl. Phys. **B126**, 298 (1977).
[29] V. N. Gribov and L. N. Lipatov, Sov. J. Nucl. Phys. **15**, 438 (1972).
[30] H. Mäntysaari and P. Zurita, Phys. Rev. D **98**, 036002 (2018).
[31] S. Uehara *et al.*, Phys. Rev. D **86**, 092007 (2012); M. Masuda *et al.*, Phys. Rev. D **93**, 032003 (2016).
[32] N. Nikolaev, J. Speth, and V. Zoller, Phys. Lett. B **473**, 157 (2000).
[33] M. Block, L. Durand, and D. W. McKay, Phys. Rev. D **79**, 014031 (2009).
[34] M. Block, L. Durand, P. Ha, and D. W. McKay, Phys. Rev. D **83**, 054009 (2011).
[35] M. M. Block, L. Durand, P. Ha, and D. W. McKay, Phys. Rev. D **84**, 094010 (2011).
[36] M. M. Block, L. Durand, P. Ha, and D. W. McKay, Phys. Rev. D **88**, 014006 (2013).
[37] G. R. Boroun and P. Ha, Phys. Rev. D **109**, 094037 (2024).
[38] P. C. Barry, C.-R. Ji, N. Sato, and W. Melnitchouk, Phys. Rev. Lett. **127**, 232001 (2021).
[39] N. Y. Cao, P. C. Barry, N. Sato, and W. Melnitchouk, Phys. Rev. D **103**, 114014 (2021).
[40] K. Golec-Biernat and S. Sapeta, J. High Energy Phys. 03 (2018) 102.